Supporting Information

Rational Design of Mesoporous NiFe-alloy-based Hybrids for Oxygen Conversion Electrocatalysts

Suqin Ci,‡ Shun Mao,‡ Yang Hou, Shumao Cui, Haejune Kim, Ren Ren, Zhenhai Wen,* Junhong Chen*

Department of Mechanical Engineering, University of Wisconsin-Milwaukee, 3200 North Cramer Street, Milwaukee, Wisconsin 53211, United States

Address correspondence to

wenzhenhai@yahoo.com, jhchen@uwm.edu

Author Contributions

‡These authors contributed equally.

Keywords: Electrocatalysts**,** Oxygen reduction reaction, Oxygen evolution reaction**,** NiFe alloy, Mesoporous

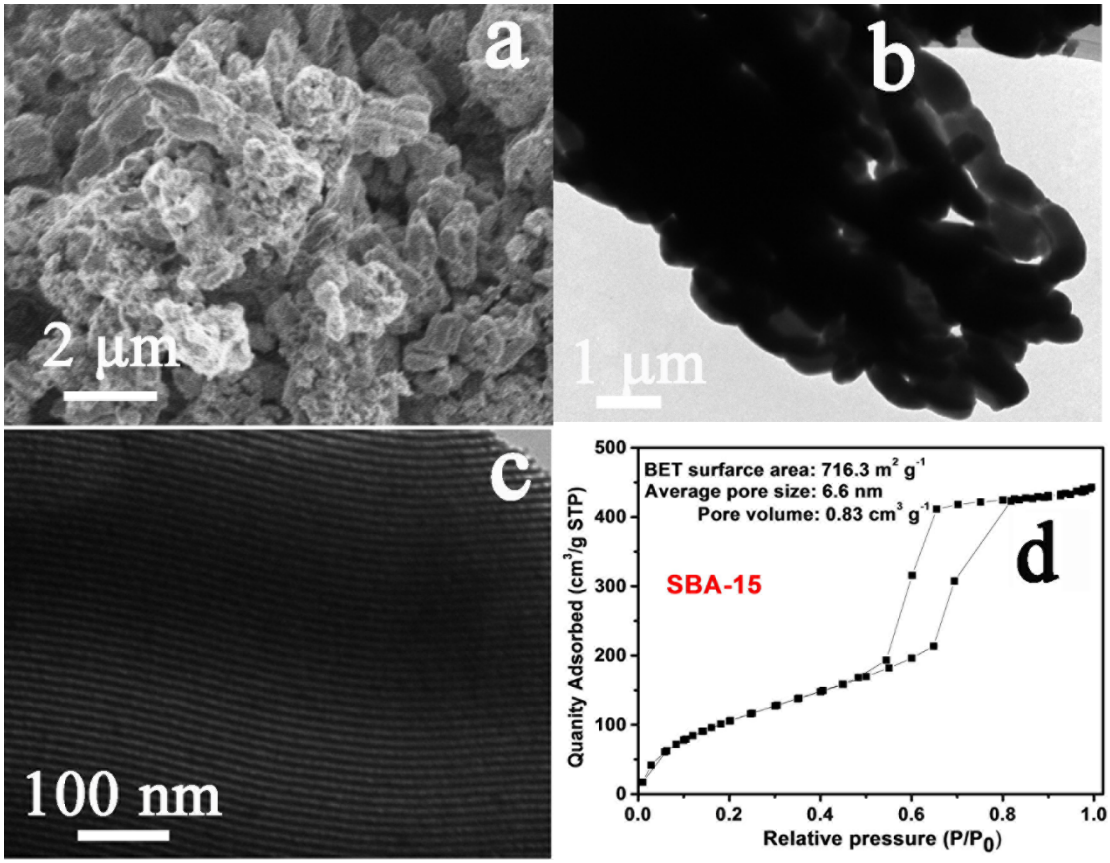

Figure S1. (a) SEM image, (b, c) TEM images, and N_2 adsorption-desorption isothermal curve of the SBA-15.

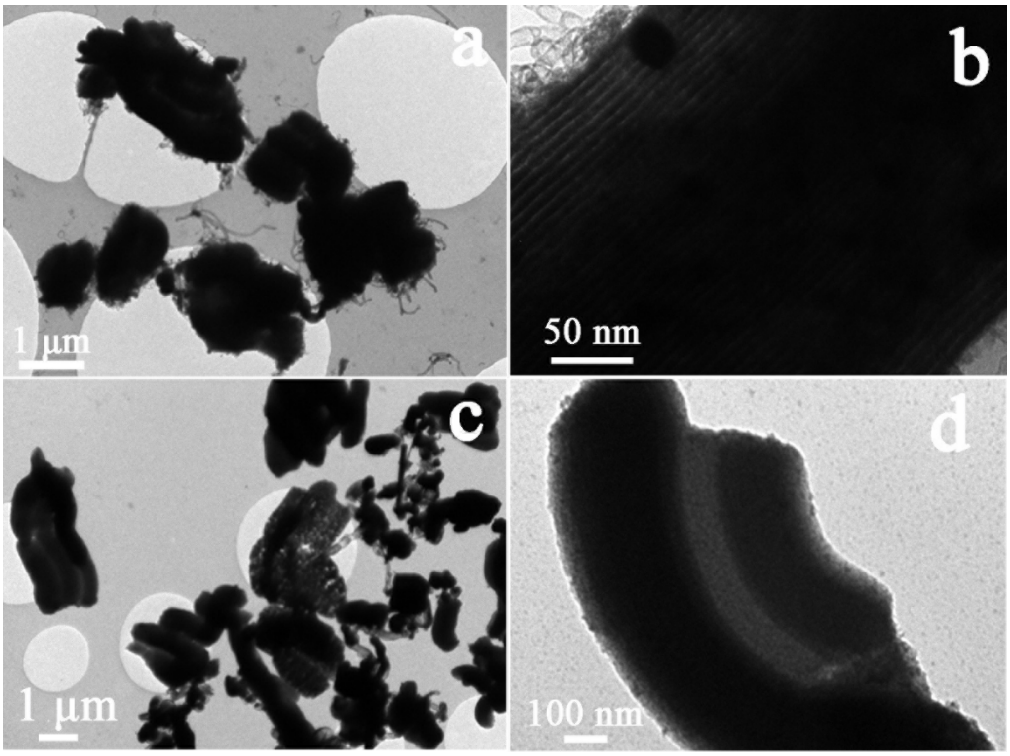

Figure S2. TEM images of (a, b) m-Ni/CN_x and (c, d) m-Fe/CN_x.

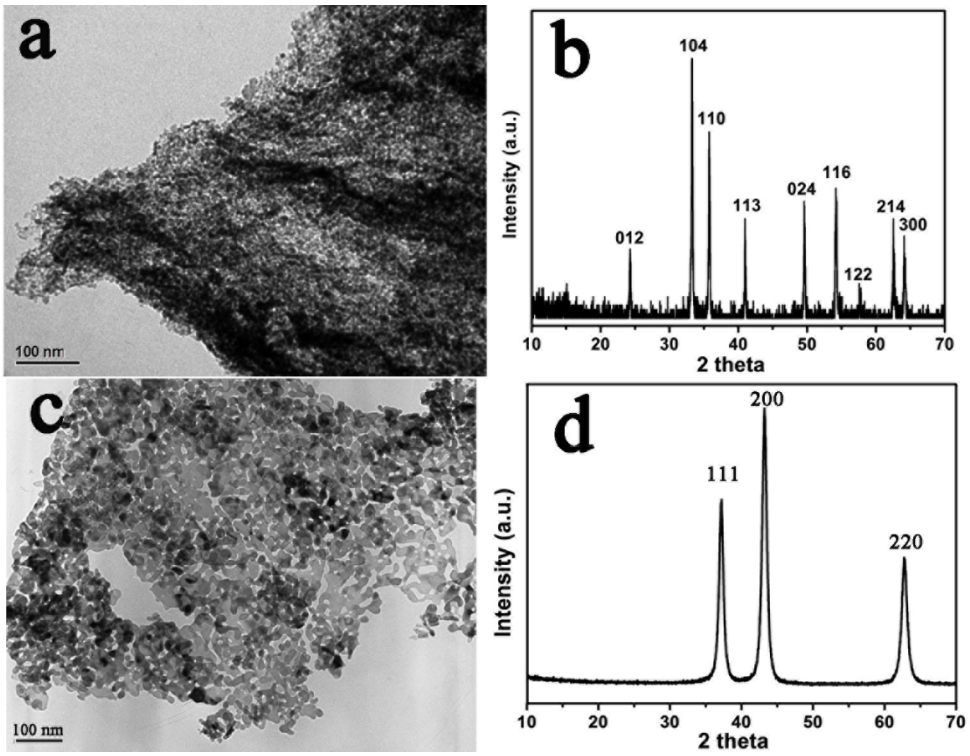

Figure S3. TEM images of (a) porous Fe_2O_3 and (c) porous NiO, and XRD pattern of (b) porous Fe_2O_3 and (d) porous NiO.

Porous Fe_2O_3 was prepared by a hydrothermal reaction with $FeCl_3$ and glucose as sources. Typically, 3.0 g glucose and 0.4 g $FeCl_3$ $6H_2O$ were added to a 30 ml aqueous solution containing ~1 mg ml^{-1} graphene oxide (GO) solution under vigorous stirring; the mixed solution was then transfer to a 40 ml Teflon-lined stainless steel autoclave and heated at 180 ºC for 5 h. After three rounds of centrifugation and washing, the resulting solid products were then converted to porous Fe_3O_4 by burning up the carbonaceous polymers and GO at 450 ºC for 3 h. Porous NiO was prepared through the method developed by us previously.[1]

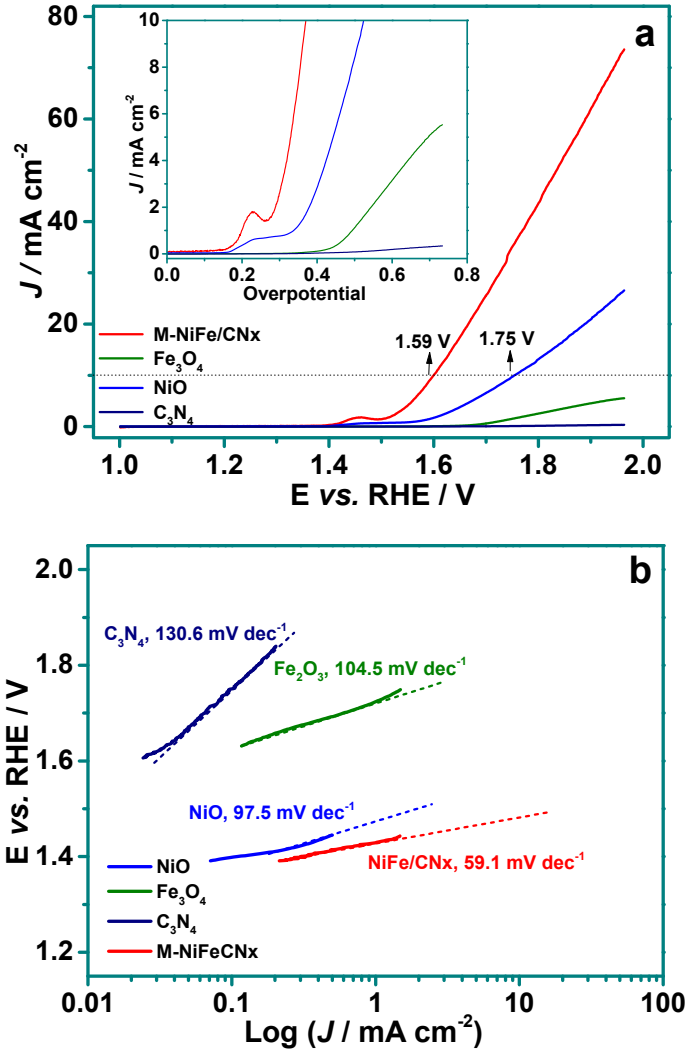

Figure S4. Rotating disk voltammograms and the corresponding data re-plotted as the current density vs. overpotential (inset) in O_2-saturated 0.1 M KOH at a scan rate of 5 mV s^{-1} and 1600 rpm, and b) the corresponding Tafel plots at the m-NiFe/CN_x, porous Fe_2O_3, porous NiO, and C_3N_4 modified electrodes.

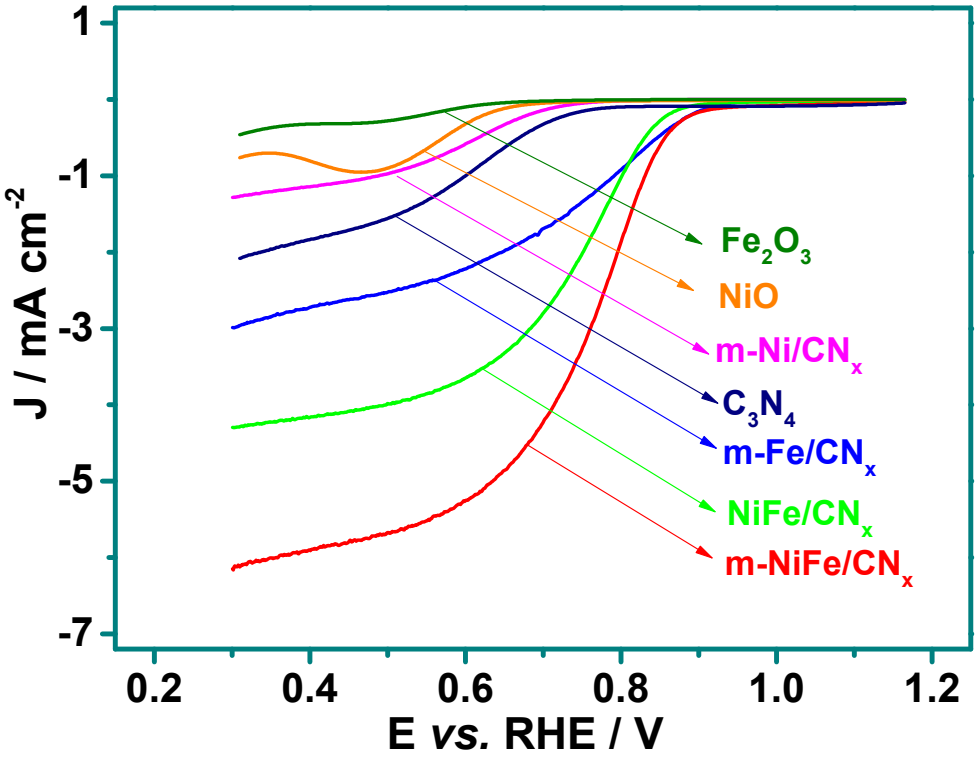

Figure S5. Linear sweep voltammetry curves of different materials modified electrode at a rotation rate of 1,600 rpm.

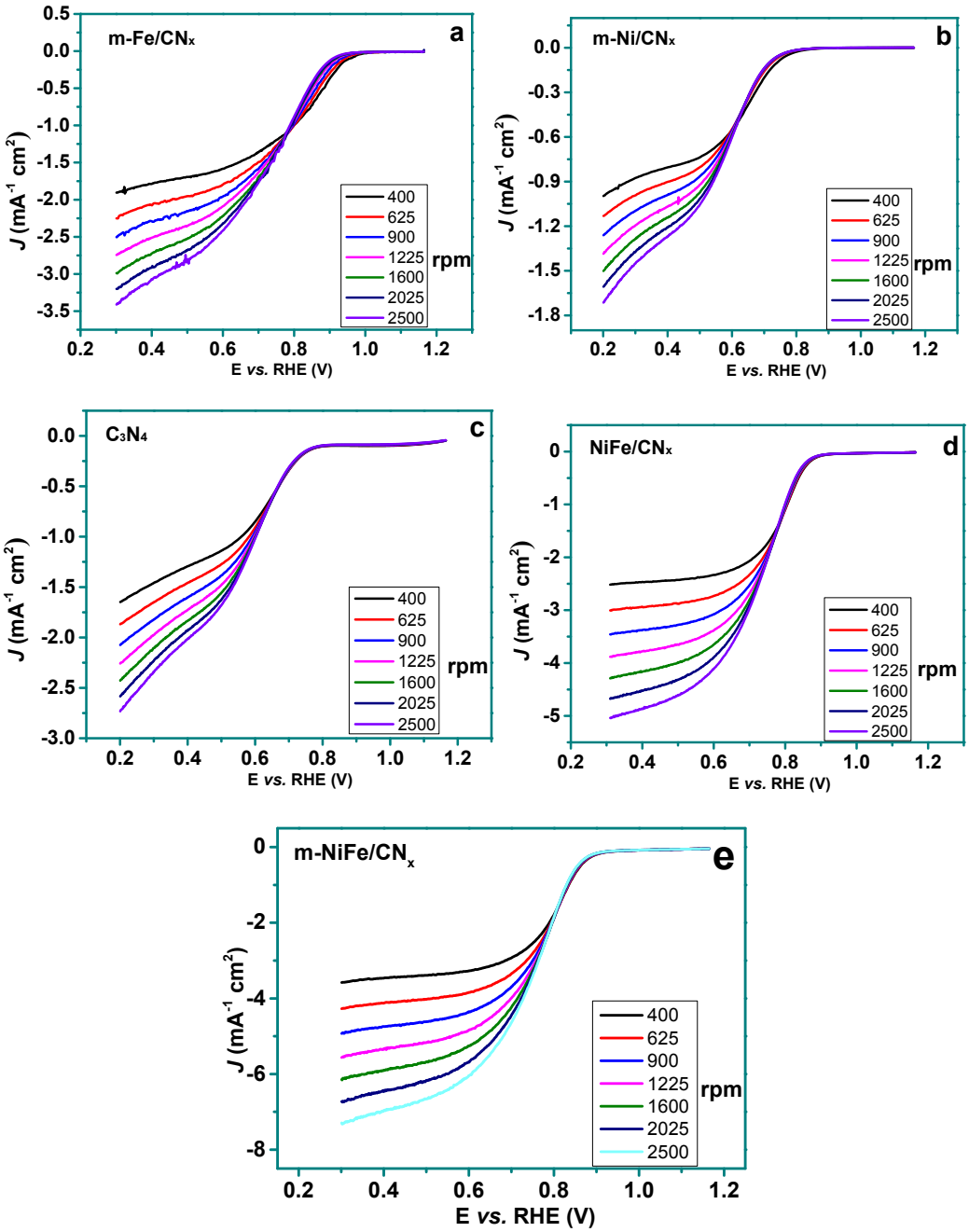

Figure S6. Polarization curves of ORR in the potential window range of 1.2~0.3 V with different rotation rates for (a) m-Fe/CN_x, (b) m-Ni/CN_x, (c) C_3N_4, (d) NiFe/CN_x, (e) m-NiFe/CN_x.

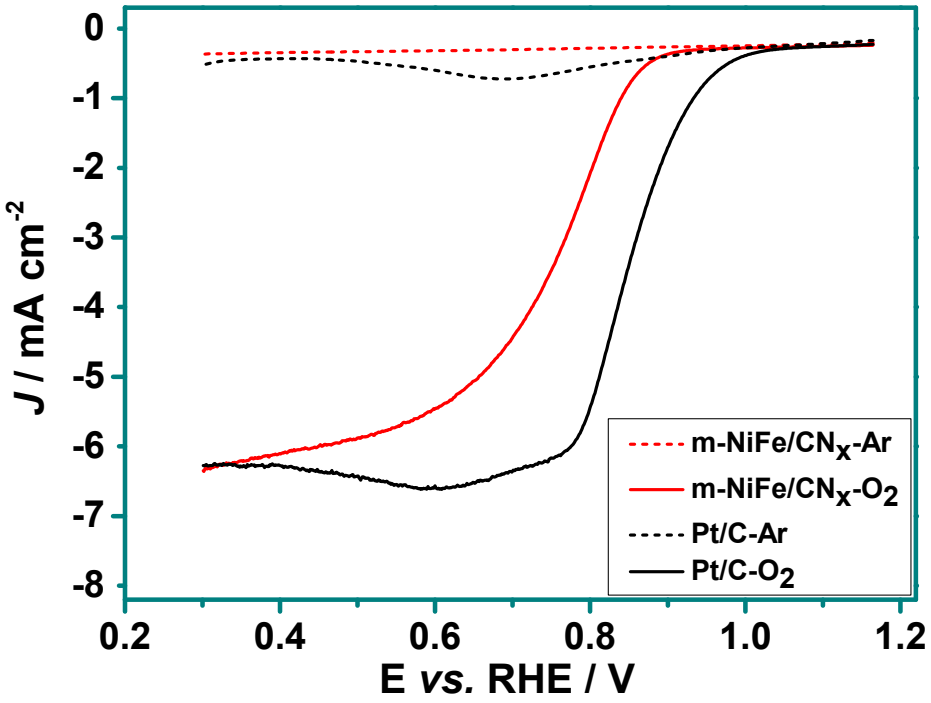

Figure S7. RDE curves of $NiFe/C_3N_4$ (red) and PtC (black) in Ar- (dash line) or O_2-saturated (solid line) 0.1 M KOH solution at a scan rate of 5 mV s^{-1} and a rotation speed of 1,600 rpm.

Table S1, S2 and S3 (Note: the potential in all tables is relative to RHE)

Table S1. Performance parameter of the bifunctional electrocatalysts for OER and ORR

Ref	Catalyst	OER			ORR			Oxygen electrode	Electrolye
		Onset potential (V)	Overpotential at 10 mA cm^{-2}	Tafel slope (mV dec^{-1})	Onset potential	Potential at 3 mA cm^{-2}	*n*	Δ (OER–ORR): *E*(V)	
This work	**m-NiFe/CNx**	**~1.45**	**0.36**	**59.1**	**0.91**	**0.76**	**~3.7**	**0.83**	**0.1 M KOH, 1600 rpm, 5 mV s^{-1}**
	NiFe/CNx	**~1.57**	**0.47**	**73.6**	**0.89**	**0.68**	**~3.2**	**1.02**	
	m-Fe/CNx	**~1.74**	**>0.7**	**102.8**	**0.91**	**0.32**	**~2.5**	**>1.5**	
	m-Ni/CNx	**~1.71**	**0.65**	**94.5**	**0.71**	**<0.3**	**1.5**	**>1.5**	
	Porous NiO	**~1.59**	**0.52**	**97.5**		**<0.3**	**2.3**	**>1.5**	
	Porous Fe_2O_3	**~1.71**	**>0.7**	**104.5**		**<0.3**	**1.8**	**>1.5**	
	C_3N_4	**>1.8**	**>0.8**	**130.6**	**0.76**	**<0.3**	**2.2**	**>1.5**	
1[2]	**$NiCo_2O_4$**	**1.56**	**0.41**	**---**	**0.84**	**~0.65**	**3.4–3.9**	**0.99**	**0.1 M KOH, 2500 rpm, 10 mV s^{-1}**
2[43]	**$NiCo_2S_4$@N/S-rGO**	**1.56**	**0.47**	**---**	**0.85**	**~0.76**	**3.6-3.8**	**0.94**	**0.1 M KOH, 1600 rpm, 5 mV s^{-1}**
3[4]	**Co_3O_4/Co_2MnO_4**	**1.55**	**0.54**	**---**	**0.87**	**0.68**	**3.97**	**1.09**	**0.1 M KOH, 1600 rpm, 5 mV s-1**
4[5]	**$CaMn_4O_x$**	**---**	**0.54**	**---**	**~0.90**	**0.73**	**---**	**1.04**	**0.1 M KOH, 1600 rpm, 5 mV s^{-1}**
5[6]	**$CoFe_2O_4$/rGO**	**1.50**	**0.48**	**---**	**~0.83**	**~0.73**	**3.8-3.9**	**0.98**	**0.1 M KOH, 1600 rpm, 10 mV s^{-1}**
6[7]	**CG–CoO**	**1.5**	**0.34**	**71**	**0.90**	**---**	**~4**	**---**	**1 M KOH, 20 mV s^{-1}**
7[8]	**Co_3O_4/rmGO**	**---**	**0.31**	**67**	**0.88**	**~0.75**		**0.79**	**0.1 M KOH, 1600 rpm, 5 mV s^{-1}**
8[9]	**$CoMn_2O_4$/PDDA-CNTs**	**---**	**0.51**	**---**	**~0.97**	**0.84**	**~4.3**	**0.85**	**0.1 M KOH, 1600 rpm, 10 mV s^{-1}**
9[10]	**Mn_2O_3**	**---**	**0.58**	**----**	**~0.90**	**0.71**	**----**	**1.10**	**0.1 M KOH, 1600 rpm, 20 mV s^{-1}**
10[11]	**NGSH**	**~1.45**	**0.40**	**83**	**0.88**	**~0.68**	**3.22**	**~0.95**	**0.1 M KOH, 1600 rpm, 5 mV s^{-1}**

Table S2. Performance parameter of OER electrocatalyst

Ref	Catalyst	OER			Electrolyte
		Onset potential	Overpotential at 10 mA cm^{-2}	Tafel slope(mV dec^{-1})	
	m-NiFe/CNx	**~1.45**	**0.36**	**59.1**	**0.1 M KOH, 1600 rpm, 5 mV s^{-1}**
11[12]	3D NF/PC/AN	1.52	0.53	---	0.1 M KOH, 5 mV s^{-1}
12[13]	$LaCoO_3$	~1.48	---	60	0.1 M KOH, 1600 rpm, 10 mV s^{-1}
13[14]	Ni–NG hybrid	~1.55	---	188.6	0.1 M KOH, 50 mV s^{-1}
14[15]	3D NiFe-LDH NP	1.46	0.35	50	0.1 M KOH, 1 mV s^{-1}
15[16]	NiFe LDH/CNT	~1.50	0.32	35	0.1 M KOH, 1600 rpm, 5 mV s^{-1}
16[17]	PNG-NiCo	~1.54	---	156	0.1 M KOH, 50 mV s^{-1}
17[18]	N/C–NiOx	~1.52	~0.5	---	0.1 M KOH, 1500 rpm, 5 mV s^{-1}
18[19]	Zn−Co−LDH	1.57	~0.54	---	0.1 M KOH, 50 mV s^{-1}
19[20]	$Zn_xCo_{3-x}O_4$	~1.50	0.32	51	1.0 M KOH, 0.5 mV s^{-1}
20[21]	$Mn_3O_4/CoSe_2$	~1.45	0.45	49	0.1 M KOH, 1600 rpm, 5 mV s^{-1}

Table S3. Comparison of the ORR performance of different catalysts.

Ref	Catalyst	ORR			Electrolyte
		Onset potential	Limiting current density at 0.3 V(mA cm^{-2})	*n*	
	m-NiFe/CNx	**0.90**	**~6.3**	**~3.7**	**0.1 M KOH, 1600 rpm, 5 mV s^{-1}**
21[22]	Co-N-GN	~0.87	~4.5	3.4–3.7	0.1 M KOH, 1600 rpm, 10 mV s^{-1}
22[23]	CoO/NCNT	0.93	3.5-4	3.9	0.1 M KOH, 1600 rpm, 5 mV s^{-1}
23[24]	SGnP	~0.74	4.8	3.3	0.1 M KOH, 1600 rpm, 5 mV s^{-1}
24[25]	C_3N_4/Carbon	~0.83	3.8	4	0.1 M KOH, 1500 rpm, 5 mV s^{-1}
25[26]	NG-900	0.92	~3.5	3.7	0.1 M KOH, 1500 rpm, 10 mV s^{-1}
26[27]	Fe_3O_4/N-GA	~0.86	~3.5	3.7−3.9	0.1 M KOH, 1600 rpm, 10 mV s^{-1}
27[28]	SNGL-20	~0.86	~4.0	3.7	0.1 M NaOH, 1600 rpm, 10 mV s^{-1}

References.

[1] S. Ci, J. Zou, G. Zeng, Q. Peng, S. Luo, Z. Wen. RSC Advances, 2012, 2, 5185–5192.

[2] C. Jin, F. L. Lu, X. C. Cao, Z. R. Yang, R. Z. Yang, J Mater Chem A 2013, 1, 12170.

[3] Q. Liu, J. T. Jin, J. Y. Zhang, Acs Appl Mater Inter 2013, 5, 5002.

[4] D. D. Wang, X. Chen, D. G. Evans, W. S. Yang, Nanoscale 2013, 5, 5312.

[5] Y. Gorlin, T. F. Jaramillo, J Am Chem Soc 2010, 132, 13612.

[6] W. Y. Bian, Z. R. Yang, P. Strasser, R. Z. Yang, J Power Sources 2014, 250, 196.

[7] S. Mao, Z. H. Wen, T. Z. Huang, Y. Hou, J. H. Chen, Energ Environ Sci 2014, 7, 609.

[8] Y. Y. Liang, Y. G. Li, H. L. Wang, J. G. Zhou, J. Wang, T. Regier, H. J. Dai, Nat Mater 2011, 10, 780.

[9] X. M. Zhai, W. Yang, M. Y. Li, G. Q. Lu, J. P. Liu, X. L. Zhang, Carbon 2013, 65, 277.

[10] K. L. Pickrahn, S. W. Park, Y. Gorlin, H.-B.-R. Lee, T. F. Jaramillo, S. F. Bent, Advanced Energy Materials 2012, 2, 1269.

[11] G.-L. Tian, M.-Q. Zhao, D. Yu, X.-Y. Kong, J.-Q. Huang, Q. Zhang, F. Wei, Small 2014, n/a.

[12] J. Wang, H.-x. Zhong, Y.-l. Qin, X.-b. Zhang, Angewandte Chemie International Edition 2013, 52, 5248.

[13] J. Suntivich, K. J. May, H. A. Gasteiger, J. B. Goodenough, Y. Shao-Horn, Science 2011, 334, 1383.

[14] S. Chen, J. Duan, J. Ran, M. Jaroniec, S. Z. Qiao, Energ Environ Sci 2013, 6, 3693.

[15] Z. Lu, W. Xu, W. Zhu, Q. Yang, L. Xiaodong, J. Liu, Y. Li, X. Sun, X. Duan, Chemical Communications 2014.

[16] M. Gong, Y. G. Li, H. L. Wang, Y. Y. Liang, J. Z. Wu, J. G. Zhou, J. Wang, T. Regier, F. Wei, H. J. Dai, J Am Chem Soc 2013, 135, 8452.

[17] S. Chen, S. Z. Qiao, Acs Nano 2013, 7, 10190.

[18] Y. Zhao, R. Nakamura, K. Kamiya, S. Nakanishi, K. Hashimoto, Nat Commun 2013, 4.

[19] X. Zou, A. Goswami, T. Asefa, J Am Chem Soc 2013, 135, 17242.

[20] X. Liu, Z. Chang, L. Luo, T. Xu, X. Lei, J. Liu, X. Sun, Chemistry of Materials 2014, 26, 1889.

[21] M.-R. Gao, Y.-F. Xu, J. Jiang, Y.-R. Zheng, S.-H. Yu, J Am Chem Soc 2012, 134, 2930.

[22] S. Jiang, C. Z. Zhu, S. J. Dong, J Mater Chem A 2013, 1, 3593.

[23] Y. Y. Liang, H. L. Wang, P. Diao, W. Chang, G. S. Hong, Y. G. Li, M. Gong, L. M. Xie, J. G. Zhou, J. Wang, T. Z. Regier, F. Wei, H. J. Dai, J Am Chem Soc 2012, 134, 15849.

[24] I. Y. Jeon, S. Zhang, L. P. Zhang, H. J. Choi, J. M. Seo, Z. H. Xia, L. M. Dai, J. B. Baek, Adv Mater 2013, 25, 6138.

[25] J. Liang, Y. Zheng, J. Chen, J. Liu, D. Hulicova-Jurcakova, M. Jaroniec, S. Z. Qiao, Angew Chem Int Edit 2012, 51, 3892.

[26] K. Parvez, S. B. Yang, Y. Hernandez, A. Winter, A. Turchanin, X. L. Feng, K. Mullen, Acs Nano 2012, 6, 9541.

[27] Z. S. Wu, S. B. Yang, Y. Sun, K. Parvez, X. L. Feng, K. Mullen, J Am Chem Soc 2012, 134, 9082.

[28] J. X. Xu, G. F. Dong, C. H. Jin, M. H. Huang, L. H. Guan, Chemsuschem 2013, 6, 493.